Coordination-Number Dependence of Magnetic Hyperfine Fields at ^{111}Cd on Ni Surfaces

K. Potzger, A. Weber, H. H. Bertschat, and W.-D. Zeitz
Bereich Strukturforschung, Hahn-Meitner-Institut Berlin GmbH, D-14091 Berlin, Germany

M. Dietrich
Technische Physik, Universität des Saarlandes, D-66041 Saarbrücken, Germany
The ISOLDE Collaboration, CERN, CH-1211 Genève 23, Switzerland
(Received 19 November 2001; published 31 May 2002)

Ferromagnetic Ni surfaces were investigated on an atomic scale using the perturbed angular correlation spectroscopy probe ^{111}Cd. A comprehensive set of data for magnetic hyperfine fields (B_{hf}) at various probe sites is presented. A field variation from -7 T in Ni bulk to the surprisingly large value of 16 T at the adatom position on Ni(111) is observed. A continuous nonlinear dependence is found, correlating the experimental B_{hf} values with the number of their nearest Ni neighbors. The data are discussed on the basis of recent calculations on B_{hf} values at sp-element impurities on ferromagnetic surfaces.

DOI: 10.1103/PhysRevLett.88.247201 PACS numbers: 75.70.Rf, 73.20.Hb, 76.80.+y

The knowledge of magnetic properties *on an atomic scale* on magnetic surfaces and at interfaces of ultrathin magnetic multilayers is becoming increasingly important in both basic research and in the field of applications such as the miniaturization of magnetic devices to smaller and smaller units [1]. In basic research the information on the variation of magnetic properties from atomic layer to atomic layer or even from atom to atom is of fundamental interest. One way to measure magnetic properties on the atomic scale is offered by the use of radioactive probe atoms and the observation of their interaction with the immediate environment. Applying hyperfine-interaction techniques, monolayer-resolved studies are possible [2,3] because of the short range of the hyperfine interaction, where essentially only the nearest neighbors (quantitatively expressed in the coordination number NN) contribute to the interaction. Nuclear methods, in particular, the perturbed angular correlation spectroscopy (PAC), have an extremely high sensitivity. In this technique, only a highly diluted amount of probe atoms (10^{-4}–10^{-5} of a monolayer) is needed. Therefore, the overall magnetic properties are not disturbed. Among the variety of magnetic interfaces, the surface of a ferromagnetic single crystal in ultrahigh vacuum (UHV) represents one of the most interesting cases. Such a surface offers a variety of different structures, e.g., terraces, steps, kinks, etc. defining the structural surface-layer roughness. Positioning the probe atoms at all sites available allows the coordination number to vary over a broad range. Magnetic properties are expected to vary considerably from structure to structure and a deep insight into the magnetic roughness of a ferromagnetic surface is obtained. In this Letter we show how magnetic properties of probe atoms on low-Miller-index surfaces of Ni(001) and Ni(111) could be measured systematically at a variety of different atomic positions. Including some single results from the literature, we present a full set of data for the coordination-number dependence of a selected magnetic property.

Magnetic hyperfine fields (B_{hf}'s) at the nuclei of probe atoms *in* or *on* ferromagnetic materials are caused by electronic spin and orbital contributions. Using the nontransition impurity Cd, a member of the $5sp$ elements, the polarization of the s electrons arising from the hybridization with the valence d electrons of the ferromagnetic host plays the dominant role in generating B_{hf}'s. For transition-element probe atoms [4,5], additional contributions would have to be taken into account which add to the complexity of the calculations, especially when magnetic properties of the host shall be extracted from the measurement of B_{hf}.

In the present experiment, the probes $^{111\mathrm{m}}$Cd and ^{111}In were positioned on Ni single crystal surfaces, which were prepared in the UHV chamber (base pressure 2×10^{-9} Pa) ASPIC (Apparatus for Surface Physics and Interfaces at CERN). Details of the experimental procedures were described earlier [6,7], in particular, how the radioactive precursors $^{111\mathrm{m}}$Cd or ^{111}In, decaying to the PAC probe ^{111}Cd, were produced; separated in the mass separator ISOLDE at CERN; and positioned onto the precleaned surfaces. We emphasize that the sample preparation is done with $^{111\mathrm{m}}$Cd or ^{111}In, whereas the hyperfine interaction measurement applying PAC (explicitly described in Ref. [8] with respect to surface experiments) is performed with the decay product ^{111}Cd. On a ferromagnetic surface, the probe nuclei with the nuclear magnetic moment $\mu = g_N \mu_N$ (g_N is the nuclear g factor; μ_N is the nuclear magneton) interact with the magnetic hyperfine field B_{hf}, and with the nuclear electric quadrupole moment Q_N, they interact with the electric field gradient (EFG). This results in the combined interaction frequency $\omega_c = \omega_c(\omega_L, \omega_Q, \eta, \alpha, \beta, \gamma)$ including the Larmor frequency

$$\omega_L = -g_N \mu_N B_{\mathrm{hf}}/\hbar\,, \tag{1}$$

and the electric quadrupole interaction frequency $\omega_Q = eQ_N V_{zz}/4I(2I-1)\hbar$, or the quadrupole coupling constant

$$\nu_Q = eQ_N V_{zz}/h\,. \tag{2}$$

The nuclear properties are taken from Ref. [9]. The orientation of the principal axis of the EFG with respect to the surface is defined by the Eulerian angles α, β, γ. The largest component of the diagonalized EFG tensor is given as V_{zz}. The asymmetry parameter $\eta = (V_{xx} - V_{yy})/V_{zz}$ vanishes for axial symmetry of the EFG which is true for terrace sites and adatoms on terraces of Ni. For steps and kinks, however, we have $0 < \eta \leq 1$. In the evaluation of the data the asymmetry parameter and the Eulerian angles α, β, γ offer valuable support for the identification of the probe sites, in addition to the magnitudes of the V_{zz} values. The PAC time spectra were measured in a four-detector array and the ratio function $R(t)$ of the count rates $C(\Theta)$ (Θ angle between the detectors) is given as

$$R(t) = 2[C(180°) - C(90°)]/[C(180°) + 2C(90°)]. \quad (3)$$

Examples of the measured ratio functions are presented in Fig. 1. The general expression describing the perturbed angular correlation for static electric and magnetic interactions on single crystals [13] is fitted to the experimental data in the form of Eq. (3). The parameters describing ω_c are calculated numerically and extracted from the fit. On a realistic surface, usually only a smaller fraction (10%–50%) of the probe atoms — deduced from the amplitudes in the PAC time spectra — comes to rest at structurally regular sites like substitutional terrace or step sites or as adatoms, etc. This is sufficient for the simultaneous parameter determination of more than one site or fraction; see the Fig. 1 caption. The balance of the different fractions depends on the temperature and the choice of the vicinal cut of the crystal (the state-of-the-art preparation procedure for clean metallic surfaces will be discussed in a forthcoming paper [10]). We have exploited these parameters in order to optimize the surface site occupation for each measurement. All results are collected in Table I. The V_{zz} values of the EFG show a strong dependence on the surface site. The different sites can be distinguished by the magnitude of the V_{zz} values, and the asymmetry parameter η and the angle β. At lower temperatures (around 40 K and below), essentially only adatom positions are occupied leading to a discrete frequency; see Fig. 1, bottom. Around 200 K, the probes have moved to steps and kinks. A distinction of the different fractions is obtained by the observation of their increase and decrease with increasing temperature. By this we follow a well established procedure for the same PAC probe with measured EFGs on similar surfaces, e.g., Ni(111) [2,12]; Cu(111), Cu(001) [8]; Pd(111) [14], Pd(001) [15]. At room temperature, the probes are incorporated into steps or even into the terraces. The latter position can be improved by annealing above 300 K; as a result see PAC spectrum Fig. 1, top. In summary, we obtained an unambiguous identification of the various impurity sites on Ni(111) and Ni(001) surfaces.

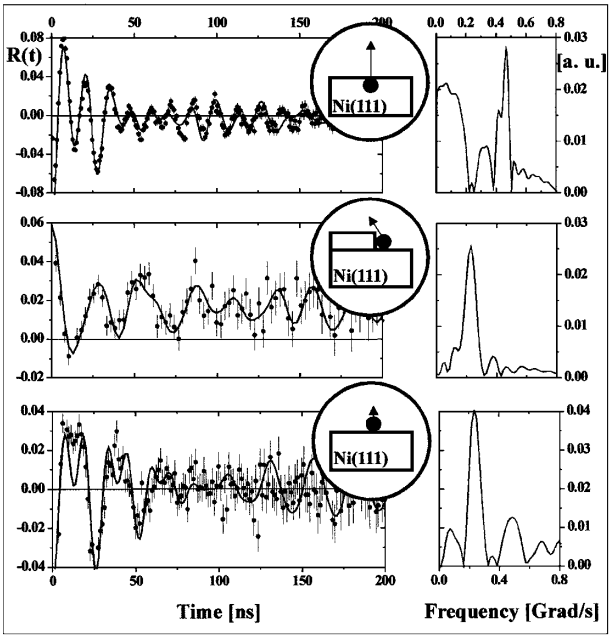

FIG. 1. PAC-time spectra of ^{111}Cd (with Fourier transforms shown on the right) at different sites on a Ni(111) surface. These selected sites are illustrated in the icons; the arrows indicate the size and the orientation of the EFG. Top: Probe atoms [40(4)%] are at substitutional terrace sites; the beat pattern is the result of the dominating electric quadrupole interaction combined with the magnetic interaction frequencies. The asymmetry parameter η vanishes because of the axial symmetry of the EFG at this site; therefore, a repetitive time pattern is observed. Center: A nonrepetitive pattern occurs at sites where the axial symmetry is lost, $0 < \eta \leq 1$. The PAC measurement represents a fraction of 22(3)% probe atoms at free kinks and 17(3)% at free steps. Bottom: Probe atoms [40(4)%] at free terrace sites (adatoms) can be observed only at low temperatures. Because of the small EFG at this site, see Table I, the magnetic hyperfine interaction is dominating and the EFG contributes to the damping of the amplitude.

We now turn to discuss the behavior of the magnetic hyperfine fields [see Eq. (1)] as the main result of this study. The B_{hf} measurements at the Ni surface were performed in external zero field in order to observe possible deviations for the direction of B_{hf} from the in-plane magnetization of Ni as it was found for Se on Ni(111) [16]. In all cases, including probe atoms at steps and kinks, the B_{hf} was found to be in plane.

The B_{hf} values are plotted versus the coordination number NN in Fig. 2; see column 3 of Table I. We have included the bulk value of Cd in Ni (NN = 12) which was measured much earlier and its sign was determined to be negative [17]. A quantitative theoretical explanation for bulk hyperfine fields was given in the 1980s [19,20], when it was found that in the beginning of the sp series the negative magnetic hyperfine fields arise from the bonding s-d hybrids below the Fermi energy. Occupied antibonding states at the Fermi energy in the middle part of the s-p series are responsible for positive hyperfine fields.

So far, no calculations exist for a whole series of measurements like the one in Fig. 2, but recently a study of magnetic hyperfine fields at substitutional and free terrace positions for the $4sp$ elements on Ni was published [5,21]:

TABLE I. Results of the ^{111}Cd-PAC measurements[a] on Ni surfaces.

Surface position	Surface orientation	Coordination number NN	T_m[b] [K]	$\lvert B_{hf}\rvert$[c] [T]	$\lvert V_{zz}\rvert$[d] [10^{17} V/cm^2]	η	β[e] [°]
In terrace[f]	(111)	9	340	6.6(2)	12.3(3)	0.0(1)	0(2)
In terrace[g]	(001)	8	300	3.5(4)	8.2(2)	0.0(1)	0
In step	(111)	7	300	4.1(5)	7.3(2)	0.7(1)	20(10)
In step[g]	(001)	7	300	3.9(4)	7.3(3)	0.6(2)	35(8)
At kink	(111)	6	180	1.0(6)	6.1(2)	0.30(5)	20(10)
At step	(111)	5	180	4.3(3)	6.7(2)	0.26(8)	48(8)
Adatom[h]	(001)	4	77	7.3(2)	0.27(3)	0	10(5)
Adatom	(111)	3	36	16.0(3)	1.0(1)	0.1(1)	0(5)

[a]All measurements were performed with ASPIC except footnote h.
[b]Measuring temperature.
[c]With $g_N = -0.306$ [9], according to Eq. (1).
[d]With $|Q_N(^{111}\mathrm{Cd})| = 0.83$ b [9], according to Eq. (2).
[e]Only β of the Eulerian angles is presented, denoting the deviation from the surface normal; the other angles depend on the vicinal cut of the single crystal, to be discussed [10].
[f]In accordance with Ref. [2].
[g]Data from Refs. [3,11].
[h]Data from Ref. [12].

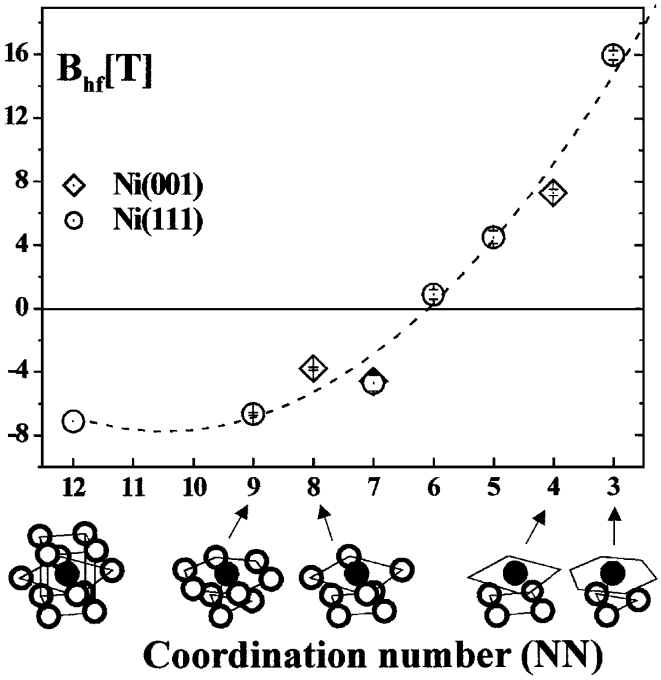

FIG. 2. Magnetic hyperfine fields (B_{hf}) at ^{111}Cd versus decreasing coordination number of Ni. Some of the coordination numbers are imaged with icons with black atoms as Cd impurities: the substitutional terrace sites for Ni(111) at NN = 9 and for Ni(001) at NN = 8; the free terrace sites for Ni(001) at NN = 4 and for Ni(111) at NN = 3, adatoms. The number NN = 7 was obtained for Ni(111) as well as for Ni(001) as substitutional step sites. The free kink site, NN = 6, and the free step site, NN = 5, were measured on Ni(111). The measurement in bulk Ni, $B_{hf} = -6.9(1)$ T [17], is included in order to start with NN = 12. The dashed line to guide the eye represents a quadratic function, $B_{hf} \sim (\mathrm{NN})^2$, to contrast any linear dependence on NN. The B_{hf} values for NN = 11, 10, which have not been measured here, might be obtained in bulk Ni performing rather complex experiments, creating vacancies by temperature quenching or irradiation; see [18].

Correlated with the reduced symmetry at the surface, in particular, at the lower coordination number NN = 4 [impurity adatom on Ni(001)], the s and p impurity states form on-site sp_z hybrids with z denoting the component perpendicular to the surface plane. Since two of such hybrids exist (outside/inside direction), a doubling of the number of bonding and antibonding states in the s density of states is obtained for the adatom. Furthermore, the reduced coordination number causes a weaker hybridization between the impurity states and the d orbitals of the Ni substrate atoms leading to a much smaller splitting of the bonding and antibonding s states. In summary, the calculations lead to a drastic change of the local density of states especially for the s electrons close to the Fermi level and consequently to a drastic change of the magnetic hyperfine fields.

Although zero field measurements do not allow a sign determination, we have assigned a change of sign in the B_{hf} values, when going from the negative bulk value to adatom hyperfine fields for the following reasons. (i) The $4sp$ series and the $5sp$ series show a very similar behavior with respect to the bulk hyperfine fields in Ni [17]. As shown in Ref. [21] for the elements in the beginning of the $4sp$ series, in particular, for Zn with a negative bulk value, the impurity hyperfine fields at the adatom position become positive with large magnitudes. Assuming a similar behavior at reduced symmetry for the $5sp$ elements, in particular, for isoelectronic Cd, we find support for the positive sign assignment for the lower coordination numbers. (ii) The substitutional terrace positions with larger NN are the closest to the bulk; therefore, a change of sign is not expected at these sites, e.g., for NN = 8, supported by *ab initio* calculations for the $4sp$ series including isoelectronic Zn [21]. (iii) Already earlier theoretical predictions [22] tentatively required a positive sign for the Cd

impurity as an adatom with NN = 3. Following these arguments, we have plotted the B_{hf} results as is shown in Fig. 2. With regard to Ref. [21], we found a continuous increase of B_{hf} versus decreasing NN. Thus we conclude that these fields reflect a *gradual* change of the local density of states, when going from the bulk to the adatom positions in several steps.

In the theoretical Refs. [21,22], magnetic hyperfine fields for $4sp$ impurities at surfaces were predicted quantitatively, exceeding the magnitude of bulk values in some cases considerably. Regarding our result for the adatom position on Ni(111) to be $B_{\mathrm{hf}} = 16$ T, we present the first experimental confirmation of such predictions — although for an element of the $5sp$ series. Because of the mobility of metallic atoms on the Ni surface with (111) orientation, such a measurement is possible only at lower temperatures; see Table I.

Two aspects deserve additional attention. First, the plot of Fig. 2 suggests that the magnetic hyperfine fields are strongly ruled by the coordination number. The easy axis of magnetization is given by the [111] direction in bulk Ni but does not play any role at the surface. This is especially confirmed at NN = 7, where B_{hf} values were obtained for both Ni orientations with the same magnitude in each case. Probe atoms on terrace sites on Ni(111) with NN = 9 and on Ni(001) with NN = 8 follow the described NN dependence. Second, in our plot the change of sign occurs at NN = 6, at the free kink site, where the impurity is outside any regular lattice site of Ni. Certainly, the size of the Cd impurity at this site has increased (which as a free atom is much larger than Ni). The change in size may have an influence on the s-electron polarization of Cd.

Summarizing, in this Letter we present a comprehensive set of magnetic hyperfine fields of Cd as a member of the $5sp$ series, measured at Ni surfaces at all positions for the coordination numbers NN between 9 and 3. The field values follow a nearly continuous increase starting with a negative bulk value and going to large adatom values. Qualitatively, this behavior can be compared with recent *ab initio* calculations for the whole $4sp$ series. The surprising prediction of B_{hf}'s at the surface, being much larger in magnitude as compared to bulk values, has been confirmed. The present results may offer a much broader basis for further calculations on the interaction of magnetically polarized substrate atoms with single nonmagnetic impurity atoms implying the calculation of the properties of a ferromagnetic surface on an atomic scale.

One of the authors, M. D., acknowledges financial support by the BMBF (05 KK1TSA/7). The authors are indebted to M. Prandolini and B. Lindgren for a critical reading of this Letter.

[1] Robert C. O'Handley, *Modern Magnetic Materials* (John Wiley & Sons, New York, 2000), p. 432.
[2] J. Voigt, X. L. Ding, R. Fink, G. Krausch, B. Luckscheiter, R. Platzer, U. Wöhrmann, and G. Schatz, Phys. Rev. Lett. **66**, 3199 (1991).
[3] H. H. Bertschat, H.-H. Blaschek, H. Granzer, K. Potzger, S. Seeger, W.-D. Zeitz, H. Niehus, A. Burchard, and D. Forkel-Wirth, Phys. Rev. Lett. **80**, 2721 (1998).
[4] H. H. Bertschat, H. Granzer, H. Haas, R. Kowallik, S. Seeger, and W.-D. Zeitz, Phys. Rev. Lett. **78**, 342 (1997).
[5] Ph. Mavropoulos, N. Stefanou, B. Nonas, R. Zeller, and P. H. Dederichs, Philos. Mag. B **78**, 435 (1998).
[6] K. Potzger, H. H. Bertschat, A. Burchard, D. Forkel-Wirth, H. Granzer, H. Niehus, S. Seeger, and W.-D. Zeitz, Nucl. Instrum. Methods Phys. Res., Sect. B **146**, 618 (1998).
[7] H. H. Bertschat, H. Granzer, K. Potzger, S. Seeger, A. Weber, W.-D. Zeitz, and Doris Forkel-Wirth, Hyperfine Interact. **129**, 475 (2000).
[8] T. Klas, R. Fink, G. Krausch, R. Platzer, J. Voigt, R. Wesche, and G. Schatz, Surf. Sci. **216**, 270 (1989).
[9] *Table of Isotopes,* edited by R. B. Firestone and V. S. Shirley (Wiley & Sons, New York, 1996), 8th ed.; $Q_N(^{111}\mathrm{Cd})$ from R. Vianden, Hyperfine Interact. **15/16**, 1081 (1983).
[10] K. Potzger, A. Weber, H. H. Bertschat, W.-D. Zeitz, and M. Dietrich (to be published).
[11] H. Granzer, Ph.D. thesis, Freie Universität Berlin, 1996 (unpublished).
[12] J. Voigt, Ph.D. thesis, Universität Konstanz, 1990 (unpublished).
[13] B. Lindgren, Hyperfine Interact. (C) **1**, 613 (1996).
[14] E. Hunger and H. Haas, Surf. Sci. **234**, 273 (1990).
[15] R. Fink, B.-U. Runge, K. Jacobs, G. Krausch, J. Lohmüller, B. Luckscheiter, U. Wöhrmann, and G. Schatz, J. Phys. Condens. Matter **5**, 3837 (1993).
[16] H. Granzer, H. H. Bertschat, H. Haas, W.-D. Zeitz, J. Lohmüller, and G. Schatz, Phys. Rev. Lett. **77**, 4261 (1996).
[17] G. N. Rao, Hyperfine Interact. **24–26**, 1119 (1985); D. A. Shirley, S. S. Rosenblum, and E. Matthias, Phys. Rev. **170**, 363 (1968).
[18] C. Hohenemser, A. R. Arends, H. de Waard, H. G. Devare, F. Pleiter, and S. A. Drentje, Hyperfine Interact. **3**, 297 (1993).
[19] J. Kanamori, H. K. Yoshida, and K. Terakura, Hyperfine Interact. **9**, 363 (1981); P. H. Dederichs, R. Zeller, H. Akai, S. Blügel, and A. Oswald, Philos. Mag. B **51**, 137 (1985).
[20] H. Akai, M. Akai, S. Blügel, B. Drittler, H. Ebert, K. Terakura, R. Zeller, and P. H. Dederichs, Prog. Theor. Phys. Suppl. **101**, 11 (1990).
[21] Ph. Mavropoulos, N. Stefanou, B. Nonas, R. Zeller, and P. H. Dederichs, Phys. Rev. Lett. **81**, 1505 (1998).
[22] B. Lindgren and A. Ghandour, Hyperfine Interact. **78**, 291 (1993).